BOREAL ENVIRONMENT RESEARCH 19 (suppl. B): 329–342 © 2014
ISSN 1239-6095 (print) ISSN 1797-2469 (online) Helsinki 30 September 2014

NanoMap: Geographical mapping of atmospheric new-particle formation through analysis of particle number size distribution and trajectory data

Adam Kristensson[1)]*, Martin Johansson[1)], Erik Swietlicki[1)], Niku Kivekäs[1)2)], Tareq Hussein[3)4)], Tuomo Nieminen[3)], Markku Kulmala[3)] and Miikka Dal Maso[5)]

[1)] *Division of Nuclear Physics, Lund University, P.O. Box 118, SE-221 00 Lund, Sweden (*corresponding author's e-mail: adam.kristensson@nuclear.lu.se)*
[2)] *Finnish Meteorological Institute (FMI), Climate Change Unit, FI-00101 Helsinki, Finland*
[3)] *Division of Atmospheric Sciences, P.O. Box 64, FI-00014 University of Helsinki, Finland*
[4)] *University of Jordan, Department of Physics, JO-11942 Amman, Jordan*
[5)] *Tampere University of Technology, Department of Physics, P.O. Box 692, FI-33101 Tampere, Finland*

Received 2 Dec. 2013, final version received 25 May 2014, accepted 14 Apr. 2014

Kristensson, A., Johansson, M., Swietlicki, E., Kivekäs, N., Hussein, T., Nieminen, T., Kulmala, M. & Dal Maso, M. 2014: NanoMap: Geographical mapping of atmospheric new-particle formation through analysis of particle number size distribution and trajectory data. *Boreal Env. Res.* 19 (suppl. B): 329–342.

Particle number size distributions at various field sites are used to identify atmospheric new-particle formation (NPF) event days. However, the spatial distribution of regionally extensive events is unknown. To remedy this situation, the NanoMap method has been developed to enable the estimation of where NPF occurs within 500 km from any field station using as input size distribution and meteorological trajectories only. Also, the horizontal extension of NPF can be determined. An open-source program to run NanoMap is available on the internet. NanoMap has been developed using as an example the Finnish field site at Hyytiälä. It shows that there are frequent NPF events over the Baltic Sea, but not as frequent as over Finland for certain wind directions; hence NanoMap is able to pinpoint areas with a low or high occurrence of NPF events. The method should be applicable to almost any field site.

Introduction

The aerosol particle number size distribution is the most important property of aerosol particles in determining their interaction with the surrounding environment. For instance, the amount of solar energy scattered by aerosol particles increases with the concentration of scattering particles, which in practice have to exceed a certain size (typically a few hundred nanometers). Cloud properties, in turn, depend on the number of aerosol particles that are large enough to act as cloud condensation nuclei (CCN). With an increase of CCN, there is a possibility that the number of small cloud droplets also increases, producing brighter clouds with a stronger cooling effect (Lohmann and Feichter 2005). Thus, to correctly estimate the effects of aerosol particles on climate, it is important to understand processes affecting aerosol particle number and size.

Editor in charge of this article: Hannele Korhonen

In many areas of the world, new nanometer-sized particles are on some days formed through a gas-to-particle formation process. These events are known as new-particle formation (NPF) events. During many NPF events, subsequent particle growth by condensation of additional gas-phase vapors lasting from hours to days has been observed (Kulmala *et al*. 2004a, Hussein *et al*. 2009). These particles have the possibility to grow to CCN sizes (Kerminen *et al*. 2005, Kerminen *et al*. 2012) and contribute to a significant fraction of global CCN (Merikanto *et al*. 2009). The duration and continuity of the NPF events implies that the secondary aerosol number formation and the growth of these particles takes place over an area with a large geographic extent (Hussein *et al*. 2009), i.e. these are regionally-extensive NPF events. The formation starts in the nanometer size range. If, at the field station, the particles are observed at a diameter larger than a few nanometers, it means that they were formed either sometime ago and grew to this larger size, or they were introduced to the atmosphere at a larger size. The continuity of the observed new growing mode makes the latter alternative highly unlikely. Since the particles were formed sometime ago, they were also formed upwind at a certain distance from the field station, and hence these NPF events do have a regional extent.

In general, both NPF and growth strongly depend on several environmental factors. The formation is strongly linked to concentrations of sulfuric acid, but also oxidation products of biogenic volatile organic carbon compounds (BVOCs), such as mono- or sesquiterpenes, which may affect the particle number production rate (Kulmala *et al*. 2013). Amines or other basic compounds may also influence formation rates (Kirkby *et al*. 2011, Almeida *et al*. 2013). The initial growth of the nanometer-sized particles is even more strongly linked to terrestrial sources of condensable organic material, with precursors emitted from vegetation being oxidized in photochemical processes (Kulmala *et al*. 2013). In the Nordic area during the warmer season, aerosol particles are likely to form in air masses arriving from the Norwegian and Barents Seas and traveling over forested land areas (Sogacheva *et al*. 2005). If the air arrives from regions that are affected by other sources, such as shipping or heavy industrial activity, we know much less about the occurrence of NPF. With better information on the spatial distribution, i.e. when and where new-particle formation takes place over a larger area and its horizontal extent, the role of anthropogenic emissions in NPF could be investigated in more detail. The spatial distribution and extent is additionally a key piece of information required to constrain the influence of NPF as a source of regional and global CCN at present and in the future.

The knowledge of NPF has been gathered mainly by means of long-term ground-level observations made at single-point field sites, which are placed hundreds or thousands of kilometers apart (Kulmala *et al*. 2004a). The occurrence of NPF at specific field sites far away from each other alone does not provide enough information to deduce where and when NPF takes place between the field sites. With the limited knowledge behind the mechanism of NPF, it is one of the reasons why regional and global modeling of NPF remains very uncertain. Nor will we ever anticipate a global coverage of field sites, which are only several tens or hundreds of kilometers apart to be able to resolve the spatial distribution of NPF.

With a direct comparison between field sites or by using meteorological back trajectories or wind data, it is at least possible to deduce the regional extent of NPF events. This opportunity has rarely been exploited. Jeong *et al*. (2010) and Crippa and Pryor (2013) found that the horizontal extent of the most extensive NPF in USA and Canada is at least on the order of hundreds of kilometers, while in Scandinavia, Hussein *et al*. (2009) noted that the extent of regionally-extensive NPF could be at least 1000 km. In central Europe, the spatial extent should be several hundreds of kilometers according to Birmili *et al*. (2003). Crippa and Pryor (2013) pointed out that within this spatial scale there is a site-to-site variability in the formation and growth rates of NPF.

To be able to determine the spatial distribution of NPF, other approaches than those mentioned above are needed. Hussein *et al*. (2009) showed

that it is feasible to use air-mass back trajectories to infer where and when NPF takes place within thousands of kilometers around the field sites.

The aim of this study was to expand on this idea and to develop a method that uses trajectories and size-distribution data from a specific field site to estimate the spatial distribution of NPF around the measurement station. There are many field sites around the world where the size distribution has been measured (Kulmala *et al*. 2004a), also for extended periods of time (Asmi *et al*. 2013). Hence, there is an opportunity to estimate spatial distributions of NPF in different areas of the globe. This calls for a method which is simple and user-friendly, and available in form of a computer program distributed through the internet.

The NanoMap method has been developed for this purpose, and a computer program to perform the NanoMap analysis with the manual is available on the internet at www.cast.lu.se/NanoMap.htm. NanoMap can be applied to those type I NPF events that show a regional extent at a single-point field site. After that, the period during which particle growth can be observed in the measured particle number size distribution spectra is recorded. If the growth can be followed from the lowest nanometer range for several hours to sizes of several tens of nanometers, it means that the grown particles were formed several hours ago upwind from the field site. Where this formation took place can be calculated using meteorological back-trajectories. With those data, a map can be plotted showing the spatial distribution of regional NPF events, i.e. the number of NPF events as a function of geographical area, even as far as 500 km away from the field station. NanoMap is intended both for short data sets — from months to a few years — to investigate where events took place, and for longer data sets of several years or longer to obtain statistics of the geographical occurrence of NPF events with dense spatial coverage and precision. Beside the spatial distribution output from NanoMap, NanoMap is also intended for the determination of the horizontal extent of an event, i.e. how far away we are able to observe an event taking place at the same time as at the field site where the size distribution is measured.

NanoMap

Basic concept

To illustrate the NanoMap method, we describe an example of its usage for a type I event registered on 12 May 2005 at the SMEAR II station at Hyytiälä, Finland (61°51´N, 24°17´E; *see* Dal Maso *et al*. 2007) (Fig. 1a). On this day, NPF was observed between roughly 08:00 and 17:00 local time at 3 nm diameter, which is the lowest detectable size of the size distribution instrument used. We could follow the growth of these particles to the size of around 40 nm count median diameter (CMD) reached at 24:00 local time. The particles ~40 nm in diameter observed at 24:00 had been formed about 7 to 16 hours earlier (24:00 – 17:00 = 7 h, and 24:00 – 08:00 = 16 h). By following the meteorological back-trajectory 7 to 16 hours backwards in time from 24:00, we estimated where the nanometer-sized particles had been formed upwind of the measurement site assuming that the formation took place at the same time upwind of the station as at the station (the simultaneous event assumption).

We also assumed that the formation starts at 1.5 nm diameter due to the cluster stabilization process, and that this is followed by a growth-activation process via condensation of gaseous precursors to larger sizes (*see* Kulmala *et al*. (2013). NanoMap is based on the type I events, which exhibit a clear growth. Hence, NanoMap is used for finding where the formation of 1.5 nm diameter particles took place only during the days when the growth to sizes larger than 1.5 nm diameter is also observed. It should be remembered, however, that these activation processes are observed in a Finnish boreal forest environment (Kulmala *et al*. 2013), and that other processes and formation diameters might be more applicable elsewhere. The current diameter choice is justified, since there are no studies reporting other diameter values at the onset of formation.

The NanoMap-method output consists of two parts:

1. *The spatial distribution of NPF at 1.5 nm*

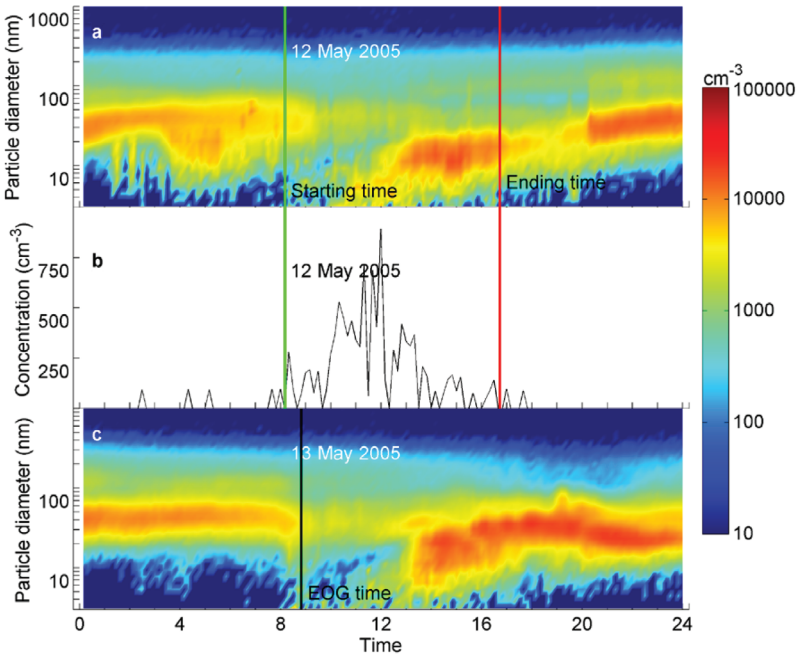

Fig. 1. An example of a type I event at SMEAR II (Hyytiälä, Finland). The green and red lines show the start (~08:00) and end (~17:00) times, respectively, of (**a**) particle number size distribution, and (**b**) particle number concentration in the lowest size bin of the DMPS instrumentation during 12 May 2005. (**c**) Particle number size distribution during 13 May 2005; the black, vertical line shows the EOG time (~09:00).

diameter up to 500 km away from a field site. NanoMap gives the source area of the formation of 1.5 nm diameter particles along certain trajectory lines. It is only applicable to areas which are upwind of the field site and can be connected to a specific event observed at the field site. We can also determine how probable it is for this source area to produce new particles but we will not get the occurrence or probability of NPF for all wind directions at a specific area, and we will not know how widespread the entire area of NPF during a specific event day is. In other words, at least for certain wind directions we can say where NPF typically takes place and where it is less likely to take place. Valuable information can be gained especially in cases where there are areas geographically close to each other, but which differ strongly in their ability to produce *in-situ* NPF; examples of such areas could be coastlines or different vegetation zones.

2. *Horizontal extension of NPF observed at the field site*. By following the growing mode of the newly-formed particles as discussed in the "EOG analysis" section below, we are able to determine how far away upwind from the field station NPF can be observed on the same day as NPF at the field site. Since we are unable to follow NPF all the way upwind of the field site, we never get a maximum horizontal extension, and we are also unable to determine the extent downwind of the field site.

Flow diagram

The NanoMap method follows 4 basic steps: (1) An event classification is performed, in which only type I events (*see* next section) are used for further analysis. During these regional NPF events, the newly formed particles are growing due to condensation for at least a few hours. (2) Using the particle number size distributions of the type I events, a manual classification is performed of the time at which the formation at the lowest size bin of the size distribution starts and ends. (3) The type I particle number size distributions are used to estimate the time when the grown nucleation mode can no longer be followed (end of growth time = EOG time). (4) A geographical map with the spatial distribution of NPF events is created based on meteorological

back-trajectories, the formation time analysis, and the EOG analysis.

Event classification

The classification of new-particle-formation events is based on the method by Dal Maso *et al*. (2005), or alternatively Vana *et al*. (2008) if data on charged particles are available. For NanoMap, one would in principle only need to include type I events in the classification. However, a full classification including other event classes (undefined days, type II events, and non-events), is recommended to be able to calculate NPF occurrence statistics.

Formation time analysis

Here, the user determines the starting and ending times of the formation event. The starting time is defined as the time when the particle number concentration in the lowest size bin of the instrumentation is increasing from a background concentration, and the ending time is defined by a decrease in the same size bin (*see* Fig. 1a and b).

Please note that an increasing amount of particles in the lowest size bin of the instrument is not always found. In such a case, the starting and ending times have to be calculated according to the lowest possible size bin of the instrument where the formation event is observed as an increasing number concentration of particles as compared with the background. It is the subjective choice of the user based on the size distribution graph to select other diameter intervals for the formation-time analysis. This issue is explained in more detail in the section "Sensitivity and uncertainties of NanoMap".

EOG analysis

In this step, the user determines the last time the grown mode during type I events can be observed, i.e., the mode which was created during the new-particle formation. The grown mode can be followed up to three days in some cases. The mode does not have to show continuous growth in the observations, but can also have flat periods. Such periods do not mean that the particles are not actually growing upwind of the field site, but it could mean that the growth rate during NPF is different during different times and at different locations upwind of the field site. This is not a problem for NanoMap, since the method does not use growth rate but the time difference between formation times and EOG time to calculate when the particles were formed.

Often the EOG time corresponds to the time when the grown mode can no longer be discerned from the background concentration or when there is a sudden shift of the air mass. One should keep in mind, that sometimes EOG does not show the end of the NPF mode but only the last point in time when we can separate it from the background particle number size distribution. In such a case, we do not know whether new-particle formation takes place beyond the corresponding locations along the trajectory.

In our example case (*see* Fig. 1c), the growth of the new particle mode could be observed until 13 May 2005, and hence the EOG time is selected for that day. Please note that the particle mode does not appear to grow during all hours of the day, i.e., it has flat periods.

In some cases the EOG time is before the ending time of the event. This can happen if the growth stops before the interruption of the formation at the lowest size bin of the instrumentation at the field site. The NanoMap method is not useful for such cases, and therefore such days should be omitted.

Number map plotting

In the final step of the process, using number size distribution and meteorological back-trajectory data, a map is created of where and how many times the formation of 1.5 nm diameter particles took place around the current measurement station.

The user needs to select how long it takes for the particles to grow from on average 1.5 nm diameter to the lowest size bin of the instrument. This information is needed in order to be able to extrapolate the observed formation

at the lowest size bins of the instrument to the actual formation that takes place around 1.5 nm diameter. Since the lowest size bin of the size distribution instrument is 3.0 nm diameter and the average growth rate for the nucleation mode particles between 1.5 and 3.0 nm diameter in Hyytiälä is around 2 nm h^{-1} (Yli-Juuti *et al*. 2011), this time-shift parameter was set to 0.75 hours in our example with the Hyytiälä data.

The growth rate during individual days is different from the average value. Hence, the choice of average growth rate is a compromise. The growth rate calculations for individual days involve time-consuming semi-manual work, and could discourage users from using the NanoMap method (an example of a growth rate calculation originally made for the size ranges above 3 nm diameter is described in Dal Maso *et al*. 2005). Please note, however, that any user still should put some effort in deducing an approximate value of the average growth rate for the lowest size bins of the size distribution data. *See* the "Sensitivity and uncertainties of NanoMap" section for a discussion of how large uncertainties that may result from the average growth rate assumption.

In our example, the EOG time was selected to be at around 09:00 on 13 May 2005 (*see* Fig. 1c), and the CMD of the grown particles at the EOG time was approximately 40 nm. Starting and ending times of the event were selected to be at 08:00 and 17:00, respectively, on 12 May (*see* Fig. 1a and b). This means that the grown particles at the EOG time had been formed as 1.5 nm diameter particles between around 17 and 26 hours earlier assuming that the starting and ending times are equal over a larger region and taking into account the 45 minutes that the particles need to grow from 1.5 to 3 nm in diameter. From the trajectory data we found the location of the air mass 17–26 hours before (*see* the red line in Fig. 2a). For the current data set, the height of the trajectory when it reaches the field station was set to 100 m. However, the user is free to choose other heights as well.

This is, however, not the only trajectory line that can be plotted for the selected event day. We can also plot the line indicating where the formation of 1.5 nm diameter particles took place for the growing mode of particles observed 1 hour earlier than the EOG time, namely on 13 May 2005 at 08:00. By repeating this, i.e. stepping one hour further backwards in time until one hour after the ending time of the event on 12 May 2005 at 17:00, we get 16 trajectory lines (thin lines in Fig. 2a) and the red line for the EOG time for this current event day (Fig. 2a). Hence, this is where the formation of 1.5 nm diameter particles took place according to the air mass back-trajectories and observations made at the Hyytiälä station during 12–13 May 2005, i.e., the red line in Fig. 2a is an example of a trajectory line based on where the formation took place, while the thin lines show all the remaining areas of formation that can be identified on a specific event day.

The formation can also be depicted in a grid-cell form with an arbitrary choice of grid-cell horizontal resolution (Fig. 2b).

NanoMap results for Hyytiälä

NanoMap was run with a 10-year dataset (27 January 1997 to 31 December 2006) from the Hyytiälä station. During these 10 years, 13.5% of the analyzable days were classified as type I days. The data coverage for this period was 94% (3411 days out of 3626). The starting and ending times were calculated for all type I NPF events (459 days). The EOG time was calculated for 95% of the type I days; erroneous data included 3 non-analyzable EOG times, and 21 cases of the EOG time being before the ending time.

The results of the NanoMap analysis of the 10-year data set from Hyytiälä cannot be presented as in Fig. 2a because many events are superimposed, especially near our receptor site at Hyytiälä. Such a graph is however, very useful for shorter data sets.

For longer data sets, the preferred presentation of results is a gridded map (*see* Fig. 3a). It shows that continental Finland grid cells with forested areas near Hyytiälä exhibit a high frequency of events as has previously been observed for the Hyytiälä forest station (Dal Maso *et al*. 2005). The role of biogenic volatile organic carbon (BVOC) in the growth of the newly-formed particles in the forest, and hence in the regionally-extensive type I events, has been documented (Kulmala *et al*. 2004b, Laaksonen *et*

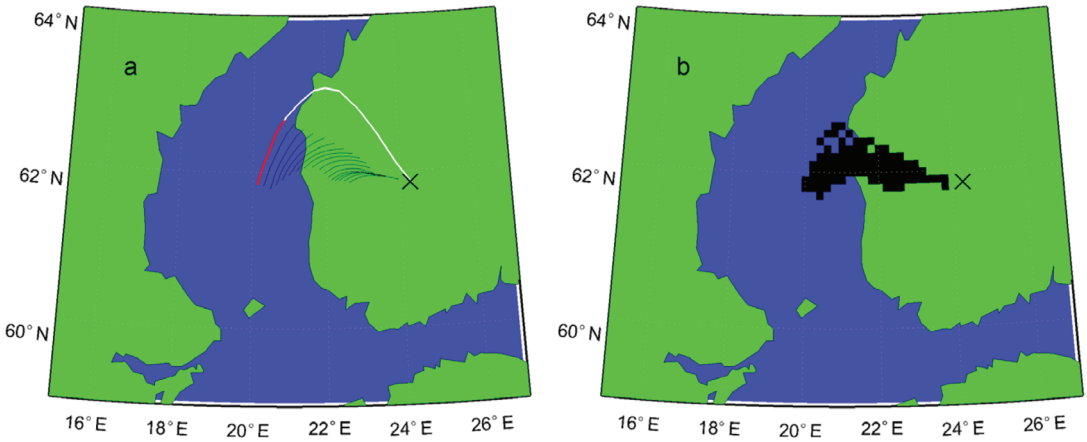

Fig. 2. (**a**) The place of formation of 1.5 nm diameter particles (red line) for the growing mode observed at the EOG time (13 May 2005, 09:00) during the type I event on 12 May 2005 at Hyytiälä (black cross). The white line shows the remaining part of the back trajectory. The thin trajectory lines show the place of formation at 1.5 nm diameter for the period between the ending time of the event and the EOG time. (**b**) The grid-cell version of **a** at the resolution of 0.1° lat. × 0.2° long., showing where the formation at 1.5 nm diameter occurred. This plot shows the number of times that we have new particles being formed over each grid cell. Please note that only one count is allowed for each grid cell during one NPF event day.

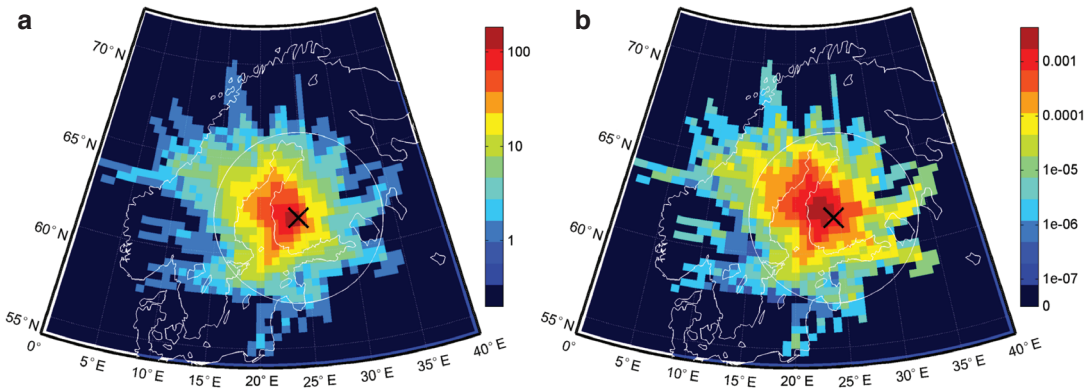

Fig. 3. (**a**) The number of times there is NPF at 1.5 nm diameter based on NanoMap results for Hyytiälä (black cross) for the years 1997–2006 with a grid resolution of 0.4° lat. × 0.8° long. (**b**) The probability of NPF events (P = NC/TC, relative scale) calculated with NanoMap for the same period and resolution. The horizontal extension of the NanoMap method 500 km from Hyytiälä is depicted with a white circle.

al. 2008). Type I events are also frequent over the northern Baltic Sea except for its northernmost tip. The wind pattern over those grid cells is dominated by northwesterly winds. However, for west-south-westerly (WSW) air masses reaching Hyytiälä, the frequency of events over the Baltic Sea is slightly lower. As these air masses arrive in Finland, the frequency is again increasing. This shows that for certain wind directions the event frequency is not as high over the Baltic Sea as it is over Finland, whereas for other wind directions it is relatively high as compared with that over Finland. Please note that the precision of NanoMap is higher within the 500-km radius from the Hyytiälä station (area within the white circle in Fig. 3a) and that the frequency of NPF is always higher closer to Hyytiälä than further away as all the trajectories meet there.

Measurements carried out on the island of Utö in the Baltic Sea (Hyvärinen *et al*. 2008) revealed that there are indeed fewer regional events over the Baltic Sea than over Finland.

Also, the longer time the air mass had spent over the Baltic Sea, the smaller the formation rate during events, indicating a lower availability of nucleating vapors. A NanoMap analysis with the Utö data is planned by the authors, in order to elucidate the location and frequency of the events over the Baltic Sea as function of air mass origin.

Much fewer events were registered east of Hyytiälä as there are fewer trajectories arriving at Hyytiälä from easterly directions. According to Nilsson *et al*. (2001) and Sogacheva *et al*. (2005) new-particle formation is generally favored by northwesterly cyclonic air-mass movements and not by easterly air masses. There are also fewer events registered south of Hyytiälä (*see* Fig. 3a). Air masses arriving from the south are more polluted and have a higher condensation sink, which decreases the possibility of observing a new particle-formation event (Sogacheva *et al*. 2008).

We evaluated that to be able to present also the probability of new-particle formation distributed over grid cells, at least 3 years of data from the Hyytiälä site are needed. Hence, we performed this analysis for a 10-year data series. By dividing the total NanoMap count in the grid cell (NC) obtained from the number-map plotting module by the total amount of trajectories passing over each grid cell during the 10 years (TC), a graph showing a factor proportional to the probability of events is produced (Fig. 3b). It clearly shows that there is a high probability of type I events over the Baltic Sea for north-westerly wind directions. There is also a lower event probability in Finland for southerly and easterly wind directions. Hence, the probability plot shows that the reason for the low number of event counts for certain wind directions in Fig. 3a is a low probability of observing events for the same wind directions.

NanoMap further gives valuable information about how far away from the station it is possible to register an event at the same time as at the field site (the extent of the formation event). As shown in Fig. 3a, the extent is approaching 1500 km. However, the larger the distance, the higher the uncertainty due to several factors as discussed in the next section. Hence, it is possible to extract only an approximate value of the extent in NanoMap. Furthermore, since the current version of NanoMap restricts the maximum EOG time to approximately 2.5 days after the event day, the true maximum extent could in some cases be higher than 1500 km.

At least in Scandinavia, NPF events often take place over areas with a horizontal extension larger than 1000 km (*see* Fig. 3a). In fact, the occurrence of events farther away than 1000 km from the field station could be even more frequent than what is shown in Fig. 3a. NanoMap systematically underestimates the EOG time during certain occasions with strong mixing with air masses from high altitudes as discussed in the next section.

Sensitivity and uncertainties of NanoMap

At least the following 7 factors can affect the precision of the NanoMap results:

1. Classification of events.
2. Choice of starting and ending times of the event.
3. Choice of EOG time.
4. Assumption that an event taking place over a larger regional area, is starting at the same time throughout this region (the simultaneous event assumption).
5. Uncertainties in trajectories.
6. Selection of grid size in the gridded map results (e.g. Fig. 3a).
7. Lowest cut-off size of the size distribution instrument.

Event classification

Since the event classification into either classes I and II depends on the discernibility of nucleation mode growth, misclassification of type II into class I is practically impossible. It could occur if a growing mode of pre-existing aerosol is confused with the NPF mode, which is very unlikely.

However, a misclassification of type I into class II could give a significant systematic underestimation of regionally-extensive NPF events. In certain studies where authors tried to calculate the growth rate of the newly formed

nucleation mode during NPF events, type I events might have been downgraded to type II events due to the difficulty of calculating the growth rate. The downgrading is in line with instructions by Dal Maso *et al*. (2005). Nevertheless, even if it is impossible to calculate the growth rate, in some of these cases it is still possible to follow the growing mode for several hours, meaning that it is a regionally extensive NPF event where NanoMap can be applied. There is however no literature record on a possible upgrade from type II to type I. Hence, we do not know how much NanoMap will be improved with the upgrading.

To reduce the underestimation, we suggest that the classification is done with a conscious bias towards class I events, so that if there is a situation when the grown mode can be followed for several hours, it should be included in the NanoMap analysis even though determination of a growth rate might be difficult.

Formation time

As soon as the particle concentration is increasing in the lowest size bin of the instrument during a type I event, the starting time of the event is assigned to this time. For the ending time, the selection is not made until the concentration in the lowest size bin approaches the lowest background values (Fig. 1a and b). The particle concentration in the nucleation mode within one hour after the starting time is normally much lower than a few hours after the starting time when there is the strongest nucleation at the field site (Fig. 1a). In the same way, the concentration within one hour of the ending time is also much lower. This means, that with these choices of starting and ending times, also areas with weak formation rates will be accounted for when creating the maps similar to the ones presented in Fig. 3a and b. This will create a smoother map of where new-particle formation takes place as compared with a case in which starting and ending times include only very high concentration values. This recommendation for the selection of starting and ending times should be followed, since otherwise weak areas of formation will not be accounted for. The aim of the NanoMap method is to include all places where formation is observed regardless of the magnitude of the formation rate.

EOG time

How far away from the measurement station new-particle formation of 1.5 nm diameter particles can be estimated during a specific event day is deduced from the EOG time. The reason for this is that the particles at the EOG time grew the longest time during the event, and hence are formed farthest away from the station, i.e., this determines the observable horizontal extent of the event. Please note that with this method it is only possible to estimate the extent if the NPF is also taking place at Hyytiälä. In some cases it can be hard to deduce a correct EOG time, and there are several possible consequences of choosing an incorrect EOG time. If an EOG time is systematically chosen too close to the ending time of the event, formation taking place far away from the station might be overlooked. On the other hand, if the EOG time is systematically chosen too far away in time from the ending time, NanoMap indicates particle formation in areas where it is not occurring. In a few cases there could be differences of more than one day for the EOG time depending on the user choice. There is also a possibility that there is a systematic problem during the selection of EOG time when winds are from a certain direction. This would systematically create large problems for a specific area.

The EOG time is a parameter with large impact on the results, and in unclear cases it is a subjective choice of the user. A large data set dilutes the effects of individual EOG times, but if the user systematically chooses early or late EOG times it affects the results. In the following sensitivity analysis, we compare NanoMap results from the cases with an early EOG time (cautious approach) and with a systematically late EOG time (less cautious approach) to investigate if these extreme choices affect the conclusions presented in the previous section.

An example of a more cautious approach is when the growing mode from the NPF event starts to fluctuate in the number concentration

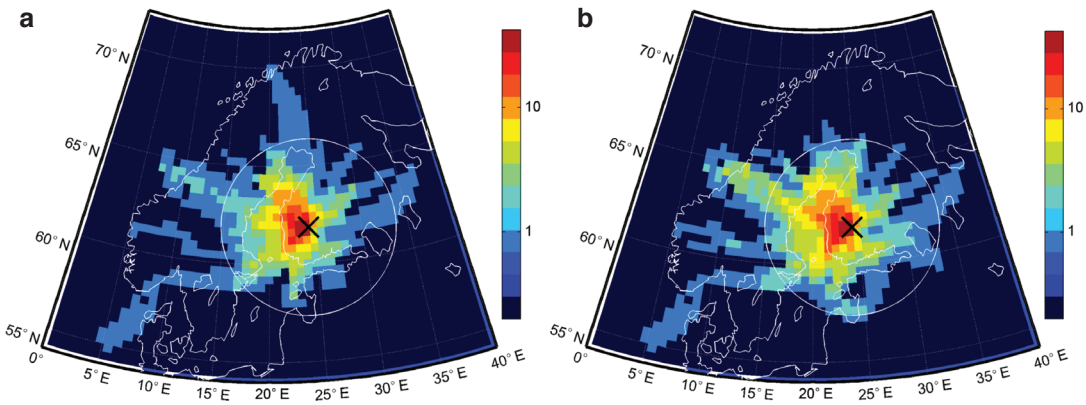

Fig. 4. Frequency of formation of 1.5 nm diameter particles according to NanoMap at Hyytiälä 2001–2002 with the (**a**) cautious and (**b**) less cautious methods of selecting EOG time (*see* the "Sensitivity and uncertainties of NanoMap" section).

or if the CMD of the growing mode is changing discontinuously, and then the user selects the EOG time before this occurs. Another example is when the growing mode from the NPF starts to merge into another particle mode with a slightly larger CMD, and the user then chooses an EOG time at the start of the merging. A less cautious approach would be to disregard the fluctuations, or to decide that it is still possible to separate the two merging modes. For these reasons, a less cautious user would possibly choose a much later EOG time than the cautious one.

The years 2001 and 2002 were selected for the EOG sensitivity analysis, since these years contain a high number of type I events. We chose a very early EOG time in the cautious analysis, and a very late EOG time in the less cautious analysis for the reasons given in the above paragraph.

The largest difference between the two analyzed cases can be seen in the events over the Baltic Sea to WSW of Hyytiälä, and at the northernmost tip of the Baltic Sea (*see* Fig. 4). The cautious approach produced fewer events over the Baltic Sea than the less cautious one, i.e., the cautious approach confirmed the conclusions in the "NanoMap results for Hyytiälä" section of slightly fewer NPF events over the Baltic Sea. The less cautious approach still shows that there are fewer events over the Baltic Sea for certain wind directions, however it is not as clear as in the cautious approach.

From the sensitivity analysis above, we can see that the cautious approach can strengthen the conclusions drawn from the base case run (Fig. 3a) by more clearly highlighting areas where formation is less likely to happen. Hence, we encourage the user to use the somewhat cautious approach even though there is no unequivocally correct or incorrect choice of EOG times.

The growing particle mode during an event can in many cases be followed until the next day. The dynamics of the lower atmosphere during the following day often result in a situation where the shallow nocturnal boundary layer breaks up in the morning, and air is entrained from above into the growing boundary layer. In the case where the nocturnal boundary layer contains the grown particles of a NPF event, this mixing often dilutes the concentration in the growing mode and may render it undistinguishable from the background concentration as in the example of EOG time in Fig. 1c. This does not mean that formation does not take place further upwind of the site as defined by the EOG time. It only means that the signature of the NPF event is not observable any more. With a typical wind speed in the boundary layer of 4–15 m s^{-1}, and with an EOG time and boundary layer break-up roughly 24 hours after the starting time of the formation, it means that we are in many cases not able to observe events that are taking place farther away than some 300–1300 km from the

station. Since these types of situations happen frequently during type I events, we limit the NanoMap analysis to roughly 500 km from the measurement station (e.g. Figs. 3 and 4). Beyond 500 km there will be an increased probability of missing a significant fraction of type I events.

The simultaneous event assumption

The NanoMap method relies on the assumption that the starting and ending times of the type I event are the same over the entire region up to 500 km upwind of the measurement station. This assumption makes it possible to calculate along which part of the trajectory the formation of 1.5 nm diameter particles takes place. This assumption, however, is certainly not valid in every situation (Hussein *et al*. 2009, Dal Maso *et al*. 2005). The times could differ between different areas due to varying conditions for nucleating vapors necessary for the new-particle formation, varying meteorological conditions, and time shifts in the sunrise. Hence, the starting and ending time assumption weakens potential local differences in the location of formation events. This weakening effect is hard to test in a sensitivity analysis with only one station. However, with a second station available within a 500 km radius from the first station, a future dedicated sensitivity analysis of this effect could be done.

Trajectory uncertainty

According to Stohl (1998), the uncertainty of the back trajectory position is about 20% of the distance traveled, which leads to a blurring effect of where the formation takes place. Furthermore, the trajectory only gives information about where the formation took place along a line, while the horizontal diffusion of air masses should reveal that the formation took place over a larger area, and the size of this area increases with increasing distance from the station (Stohl 1998). Further, the trajectories have an uncertainty in the vertical direction as well (Stohl 1998). Therefore, it is also reasonable to stop following the trajectories for more than 500 km.

Further, there is a higher probability that events taking place beyond 500 km from the station are associated with a higher air mass speed, since there is often not enough time for slower air masses to reach the station before the EOG time has passed. Hence, relatively fewer of the lower air mass speed events will be registered outside the 500 km limit. It is not justified to highlight only high wind speed events outside 500 km. Conversely, inside 500 km, a high fraction of both types of events, i.e., with low and high wind speeds are registered by the NanoMap method.

In the results presented here, 100 m as ending trajectory height was chosen. If the formation takes place above 100 m, and above the boundary layer, the origin of the formation events as deduced from NanoMap might be incorrect. Namely, trajectories above the boundary layer might be completely different from trajectories within the boundary layer. However, the Hyytiälä station NPF events have been documented to take place within the boundary layer (Kulmala *et al*. 2013), justifying the choice of 100 m in the Hyytiälä case. At stations surrounded by complex topography (e.g. mountain range) choosing correct trajectory height can be difficult, since the topography is typically not represented well enough in models that calculate the trajectories, and local altitude differences can be large. One should be cautious when using NanoMap for such areas.

Grid size

A suitable grid resolution should be chosen for a gridded map (as in Fig. 3) with a focus on the geographical features that could affect NPF in the studied area. However, one should keep in mind that a small grid box lowers the NPF counts in it, which may reduce the statistical significance of the analysis. In the Hyytiälä example (*see* Fig. 3), a 0.4° lat. × 0.8° long. resolution was sufficiently high to allow for a smoother looking plot. However, we want to remind the user that a balance between improved statistics and geographical representativeness should be aimed for.

The lowest cut-off size

The lowest cut-off size of the size distribution instrument at Hyytiälä is 3 nm diameter. Using a median growth rate of about 2 nm h^{-1} for Hyytiälä (Yli-Juuti *et al*. 2011), it takes about 45 minutes for the particles to grow from the point of formation at 1.5 nm diameter to 3 nm diameter. However, the growth rate is not always equal to 2 nm h^{-1} for individual days. Hence, the cut-off size limitation creates an uncertainty of the starting and ending time of formation, which increases with increasing cut-off size of the instrument. Therefore, we suggest whenever possible to use a cut-off size of 3 nm diameter or smaller for a reliable investigation of new-particle formation.

In addition, if the lowest cut-off size is greater than 15 nm diameter, there will be fewer days classified as event days. Hence, it will be difficult to perform NanoMap on this kind of data. Nevertheless, if the user wants to know whether formation takes place over an area that was previously not investigated, a few type I days should be sufficient for a NanoMap analysis.

Concluding remark about uncertainties

There are blurring effects due to uncertainties in event classification, selection of starting and ending times, simultaneous event assumption, and trajectory uncertainty. These added together might significantly mask local differences in the number of times new-particle formation events take place as function of geographical position. However, as seen in Fig. 3, not all patterns are smoothed out. Local differences of where and how often formation occurs are clearly discernible.

Conclusions

With the NanoMap method using measured particle number size distribution at a field site and meteorological air-mass back trajectories, new-particle formation responsible for a significant fraction of regional CCN concentration can be identified as function of geographical position as far as 500 km away from the field site. This provides an opportunity to identify where new-particle formation takes place without measurements at the place of formation, and to validate global aerosol particle models of new-particle formation over a larger area. The horizontal extent of formation events can also be deduced. NanoMap can be applied anywhere where the size distribution was measured and is useful for both small data sets where new-particle formation was not previously studied, and for larger data sets of several years, where NanoMap identifies "hot" and "low spots" of formation. NanoMap can be used at almost all field sites in the world.

Acknowledgments: The Swedish research council FORMAS, under the grant 2010-850, the Nordforsk Nordic Top-level Research initiative CRAICC: Cryosphere-atmosphere interactions in a changing Arctic climate, The Academy of Finland Centre of Excellence program (project no. 1118615), and ERC-Advanced "ATMNUCLE" (grant no. 227463) are acknowledged for financial support. The study is a contribution also to the Swedish Strategic Research Areas: Modelling the Regional and Global Earth System (MERGE), the European Seventh Framework Program, ACTRIS (EU INFRA-2010-1.1.16-262254), **A**erosols, **C**louds, and **T**race gases **R**esearch **I**nfra **S**tructure Network. Finally Peter Tunved is acknowledged for helping with creating the Hysplit meteorological back trajectories needed for the NanoMap analysis and Vilhelm Berg-Malmborg for modifications in the Matlab code of NanoMap.

References

Almeida J., Schobesberger S., Kürten A., Ortega I.K., Kupiainen-Määttä O.,, Praplan A.P., Adamov A., Amorim A., Bianchi F., Breitenlechner M., David A., Dommen J., Donahue N.M., Downard A. Dunne E., Duplissy J., Ehrhart S., Flagan R.C., Franchin A., Guida R., Hakala J., Hansel A., Heinritzi M., Henschel H., Jokinen T., Junninen H., Kajos M., Kangasluoma J., Keskinen H., Kupc A., Kurtén T., Kvashin A.N., Laaksonen A., Lehtipalo K., Leiminger M., Leppä J., Loukonen V., Makhmutov V., Mathot S., McGrath M.J., Nieminen T., Olenius T., Onnela A., Petäjä T., Riccobono F., Riipinen I., Rissanen M., Rondo L., Ruuskanen T., Santos F.D., Sarnela N., Schallhart S., Schnitzhofer R., Seinfeld J.H., Simon M., Sipilä M., Stozhkov Y., Stratmann F., Tomé A., Tröstl J., Tsagkogeorgas G., Vaattovaara P., Viisanen Y., Virtanen A., Vrtala A., Wagner P.E., Weingartner E., Wex H., Williamson C., Wimmer D., Ye P., Yli-Juuti T., Carslaw K.S., Kulmala M., Curtius J., Baltensperger U., Worsnop D.R., Vehkämäki H. & Kirkby J. 2013. Molecular under-

standing of sulphuric acid-amine particle nucleation in the atmosphere. *Nature* 502: 359–363.

Asmi A., Collaud Coen M., Ogren J.A., Andrews E., Sheridan P., Jefferson A., Weingartner E., Baltensperger U., Bukowiecki N., Lihavainen H., Kivekäs N., Asmi E., Aalto P.P., Kulmala M., Wiedensohler A., Birmili W., Hamed A., O'Dowd C., Jennings S.G., Weller R., Flentje H., Fjaeraa A.M. Fiebig M., Myhre C.L., Hallar A.G., Swietlicki E., Kristensson A. & Laj P. 2013. Aerosol decadal trends — Part 2: *in-situ* aerosol particle number concentrations at GAW and ACTRIS stations. *Atmos. Chem. Phys.* 13: 895–916.

Birmili W., Berresheim H., Plass-Dülmer C., Elste T., Gilge S., Wiedensohler A. & Uhrner U. 2003. The Hohenpeissenberg aerosol formation experiment (HAFEX): a long-term study including size-resolved aerosol, H_2SO_4, OH, and monoterpenes measurements. *Atmos. Chem. Phys.* 3: 361–376.

Crippa P. & Pryor S.C. 2013. Spatial and temporal scales of new particle formation events in eastern North America. *Atmos. Environ.* 75: 257–264.

Dal Maso M., Kulmala M., Riipinen I., Wagner R., Hussein T., Aalto P.P. & Lehtinen K.E.J. 2005. Formation and growth of fresh atmospheric aerosols: eight years of aerosol size distribution data from SMEAR II, Hyytiälä, Finland. *Boreal Env. Res.* 10: 323–336.

Dal Maso M., Sogacheva L., Aalto P.P., Riipinen I., Komppula M., Tunved P., Korhonen L., Suur-Uski V., Hirsikko A., Kurtén T., Kerminen V.-M., Lihavainen H., Viisanen Y., Hansson H.-C. & Kulmala M. 2007. Aerosol size distribution measurements at four Nordic field stations: identification, analysis and trajectory analysis of new particle formation bursts. *Tellus* 59B: 350–361.

Hussein T., Junninen H., Tunved P., Kristensson A., Dal Maso M., Riipinen I., Aalto P.P., Hansson H.-C., Swietlicki E. & Kulmala M. 2009. Time span and spatial scale of regional new particle formation events over Finland and southern Sweden. *Atmos. Chem. Phys.* 9: 4699–4716.

Hyvärinen A.P., Komppula M., Engler C., Kivekäs N., Kerminen V.-M., Dal Maso M., Viisanen Y. & Lihavainen H. 2008. Atmospheric new particle formation at Utö, Baltic Sea 2003–2005. *Tellus* 60B: 345–352.

Jeong C.-H., Evans G.J., McGuire M.L., Chang, R.Y.-W., Abbatt, J.P.D., Zeromskiene K., Mozurkewich M., Li S.-M. & Leaitch W.R. 2010. Particle formation and growth at five rural and urban sites. *Atmos. Chem. Phys.* 10: 7979–7995.

Kerminen V.-M., Lihavainen H., Komppula M., Viisanen Y. & Kulmala M. 2005. Direct observational evidence linking atmospheric aerosol formation and cloud droplet activation. *Geoph. Res. Letters* 32, L14803, doi:10.1029/2005GL023130.

Kerminen V.-M., Paramonov M., Anttila T., Riipinen I., Fountoukis C., Korhonen H., Asmi E., Laakso L., Lihavainen H., Swietlicki E., Svenningsson B., Asmi A., Pandis S.N., Kulmala M. & Petäjä T. 2012. Cloud condensation nuclei production associated with atmospheric nucleation: a synthesis based on existing literature and new results. *Atmos. Chem. Phys.* 12: 12037–12059.

Kirkby J., Curtius J., Almeid J., Dunne E., Duplissy J., Ehrhart S., Franchin A., Gagné S., Ickes L., Kürten A., Kupc A., Metzger A., Riccobono F., Rondo L., Schobesberger S., Tsagkogeorgas G., Wimmer D., Amorim A., Bianchi F., Breitenlechner M., David A., Dommen J., Downard A., Ehn M., Flagan R.C., Haider S., Hansel A., Hauser D., Jud W., Junninen H., Kreissl F., Kvashin A., Laaksnen A., Lehtipalo K., Lima J., Lovejoy E.R., Makhmutov V., Mathot S., Mikkilä J., Minginette P., Mogo S., Nieminen T., Onnela A., Pereira P., Petäjä T., Schnitzhofer R., Seinfeld J.H., Sipilä M., Stozhkov Y., Stratmann F., Tomé A., Vanhanen J., Viisanen Y., Vrtala A., Wagner P.E., Walther H., Weingartner E., Wex H., Winkler P.M., Carslaw K.S., Worsnop D.R., Baltensperger U. & Kulmala M. 2011. Role of sulphuric acid, ammonia and galactic cosmic rays in atmospheric aerosol nucleation. *Nature* 476: 429–433.

Kulmala M., Vehkamäki H., Petäjä T., Dal Maso M., Lauri A., Kerminen V.-M., Birmili W. & McMurry P.H. 2004a. Formation and growth rates of ultrafine atmospheric particles: a review of observations. *Aerosol Sci.* 35: 143–176.

Kulmala M., Suni T., Lehtinen K.E.J., Dal Maso M., Boy M., Reissell A., Rannik Ü., Aalto P., Keronen P., Hakola H., Bäck J., Hoffmann T., Vesala T. & Hari P. 2004b. A new feedback mechanism linking forests, aerosols, and climate. *Atmos. Chem. Phys.* 4: 557–562.

Kulmala M., Kontkanen J., Junninen H., Lehtipalo K., Manninen H.E., Nieminen T., Petäjä T., Sipilä M., Schobesberger S., Rantala P., Franchin A., Jokinen T., Järvinen E., Äijälä M., Kangasluoma J., Hakala J., Aalto P.P., Paasonen P., Mikkilä J., Vanhanen J., Aalto J., Hakola H., Makkonen U., Ruuskanen T., Mauldin R.L.III, Duplissy J., Vehkamäki H., Bäck J., Kortelainen A., Riipinen I., Kurtén T., Johnston M.V., Smith J.N., Ehn M., Mentel T.F., Lehtinen K.E.J., Laaksonen A., Kerminen V.-M. & Worsnop D.R. 2013. Direct observations of atmospheric aerosol nucleation. *Science* 339: 943–946.

Laaksonen A., Kulmala M., O'Dowd C.D., Joutsensaari J., Vaattovaara P., Mikkonen S., Lehtinen K.E.J., Sogacheva L., Dal Maso M., Aalto P., Petäjä T., Sogachev A., Yoon Y.J., Lihavainen H., Nilsson D., Facchini M.C., Cavalli F., Fuzzi S., Hoffmann T., Arnold F., Hanke M., Sellegri K., Umann B., Junkermann W., Coe H., Allan J.D., Alfarra M.R., Worsnop D.R., Riekkola M.-L., Hyötyläinen T. & Viisanen Y. 2008. The role of VOC oxidation products in continental new particle formation. *Atmos. Chem. Phys.* 8: 2657–2665.

Lohmann U. & Feichter J. 2005. Global indirect aerosol effects: a review. *Atmos. Chem. Phys.* 5: 715–737.

Merikanto J., Spracklen D.V., Mann G.W., Pickering S.J. & Carslaw K.S. 2009. Impact of nucleation on global CCN. *Atmos. Chem. Phys.* 9: 8601–8616.

Nilsson E.D., Rannik Ü., Kulmala M., Buzorius G. & O'Dowd C.D. 2001. Effects of continental boundary layer evolution, convection, turbulence and entrainment, on aerosol formation. *Tellus* 53B: 441–461.

Sogacheva L., Dal Maso M., Kerminen V.-M. & Kulmala M. 2005. Probability of nucleation events and aerosol particle concentration in different air mass types arriving at Hyytiälä, southern Finland, based on back trajectories analysis. *Boreal Env. Res.* 10: 479–491.

Sogacheva L., Saukkonen L., Nilsson E.D., Dal Maso M., Schultz D.M., de Leeuw G. & Kulmala M. 2008. New aerosol particle formation in different synoptic situations at Hyytiälä, Southern Finland. *Tellus* 60B: 485–494.

Stohl A. 1998. Computation, accuracy and applications of trajectories — a review and bibliography. *Atmos. Environ.* 32: 947–966.

Vana M., Ehn M., Petäjä T., Vuollekoski H., Aalto P., de Leeuw G., Ceburnis D., O'Dowd C.D. & Kulmala M. 2008. Characteristic features of air ions at Mace Head on the west coast of Ireland. *Atmos. Res.* 90: 278–286.

Yli-Juuti T., Nieminen T., Hirsikko A., Aalto P.P., Asmi E., Hõrrak U., Manninen H.E., Patokoski J., Dal Maso M., Petäjä T., Rinne J., Kulmala M. & Riipinen I. 2011. Growth rates of nucleation mode particles in Hyytiälä during 2003–2009: variation with particle size, season, data analysis method and ambient conditions. *Atmos. Chem. Phys.* 11: 12865–12886.